Multiscale study of the chiral self-assembly of cellulose nanocrystals during frontal ultrafiltration

S. Mandin, L. Metilli, M. Karrouch, D. Bleses, C. Lancelon-Pin, W. Chèvremont, E. Paineau, J.-L. Putaux, N. Hengl, B. Jean, and F. Pignon

Supplementary data

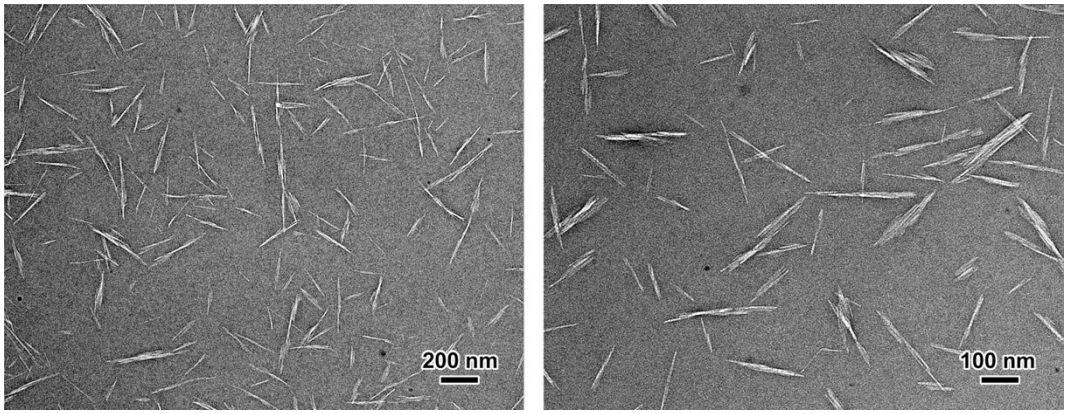

Figure S1: TEM images of a negatively stained preparation from a dilute CNC suspension.

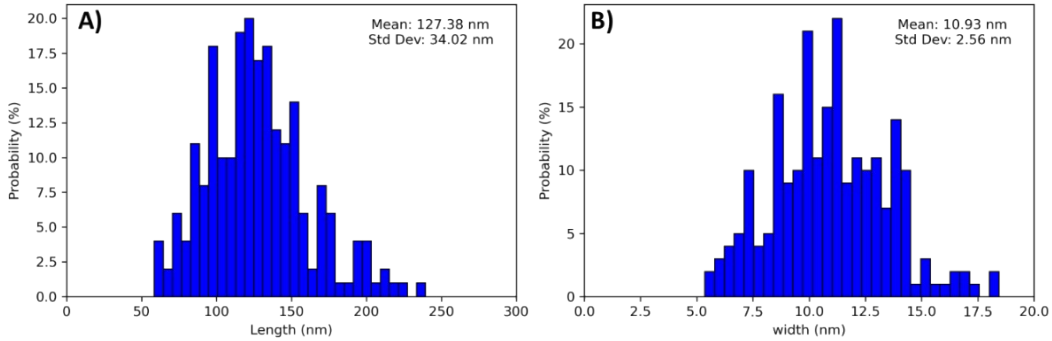

Figure S2: Length (A) and width (B) distribution histograms of the CNCs measured from the TEM images.

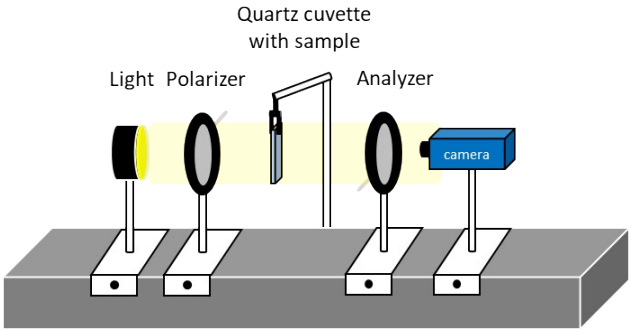

Figure S3: Cross-polarizer measurement setup.

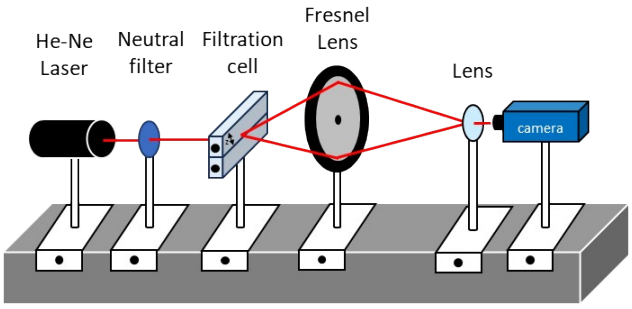

Figure S4: Scheme of the SALS setup coupled with the filtration cell.

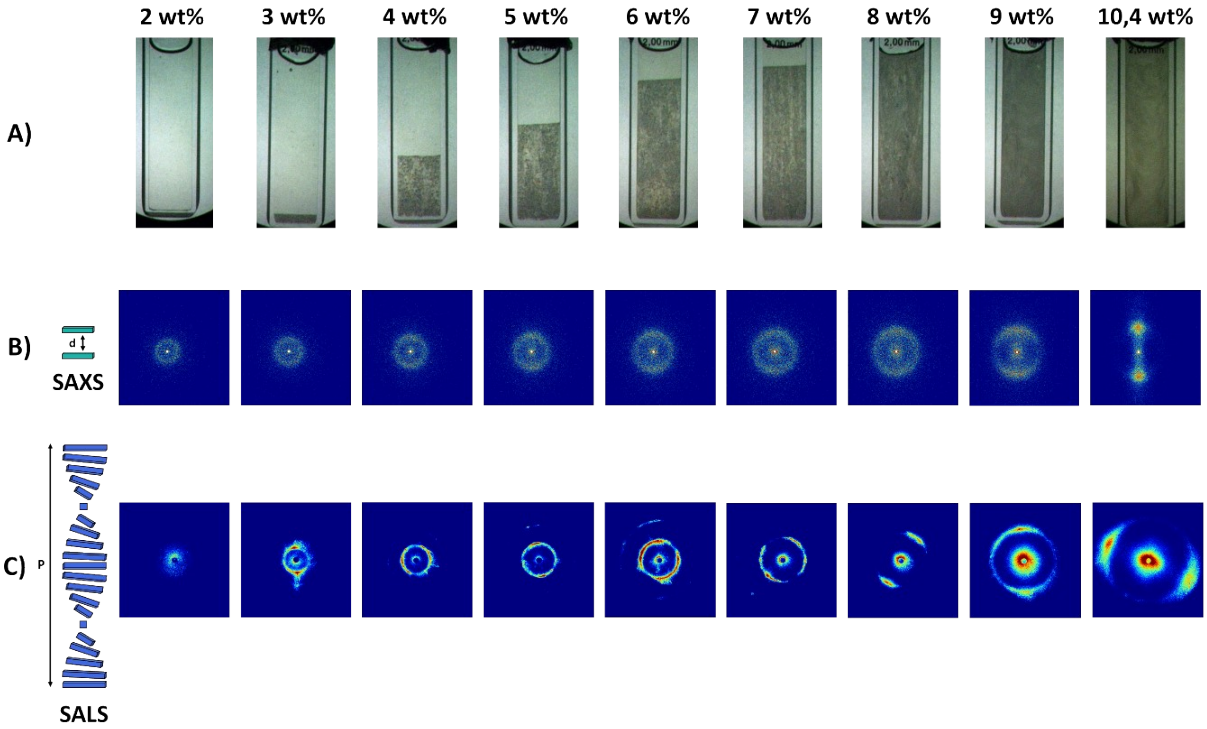

Figure S5: A) observations between cross-polarizers of CNC suspensions with increasing concentration; B) corresponding 2D SAXS patterns and C) 2D SALS patterns of the CNC suspensions recorded in the anisotropic phase.

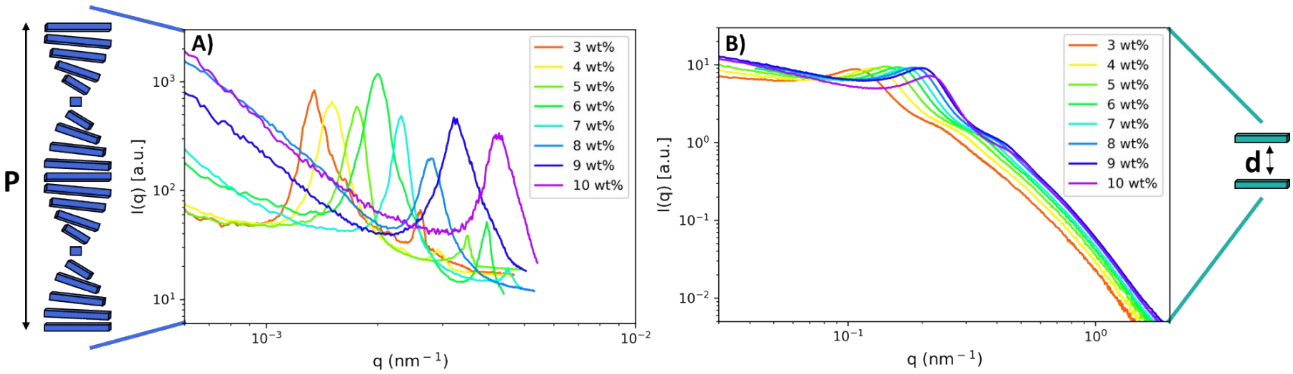

Figure S6: CNC I(q) curves obtained from SALS (A) and SAXS (B) measurements at rest.

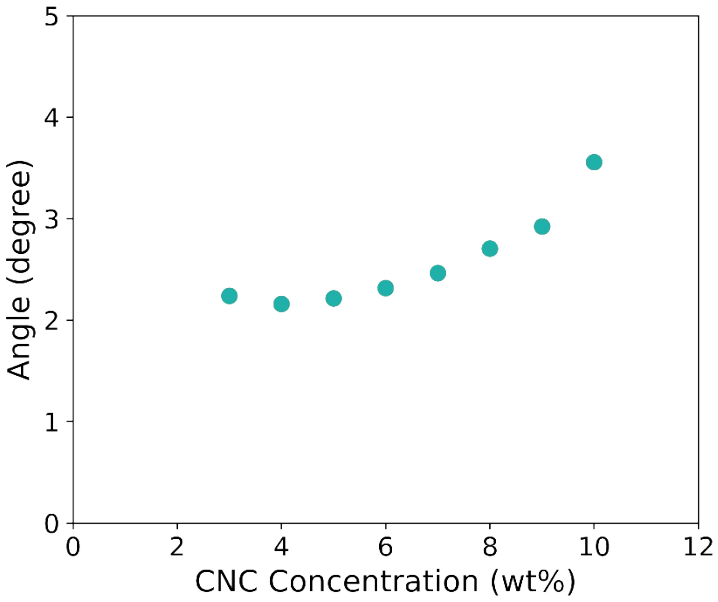

Figure S7: Rotation angle of the CNCs in the cholesteric structures as a function of concentration.

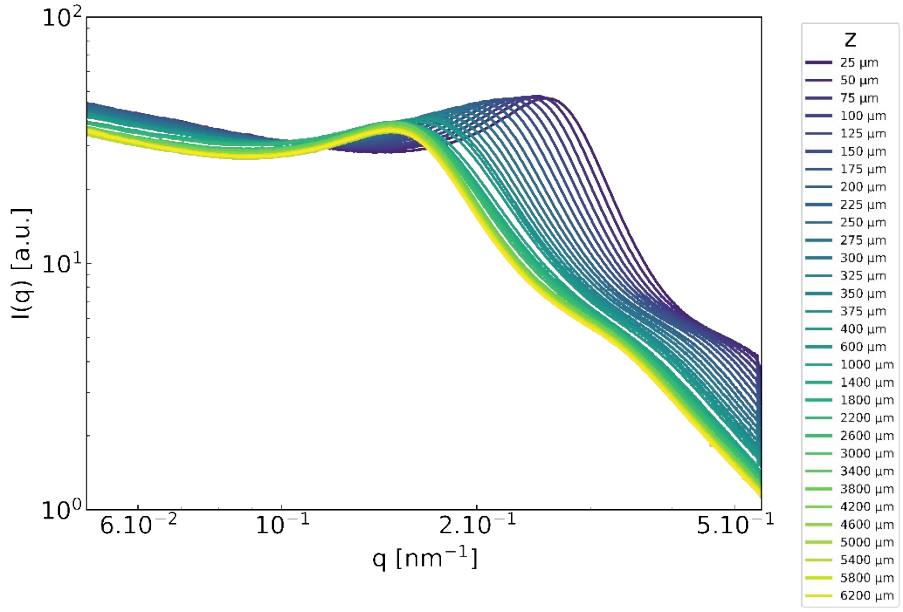

Figure S8: I(q) SAXS curve: concentration profile in the 23-min pressure deposit, 6 wt% CNCs.

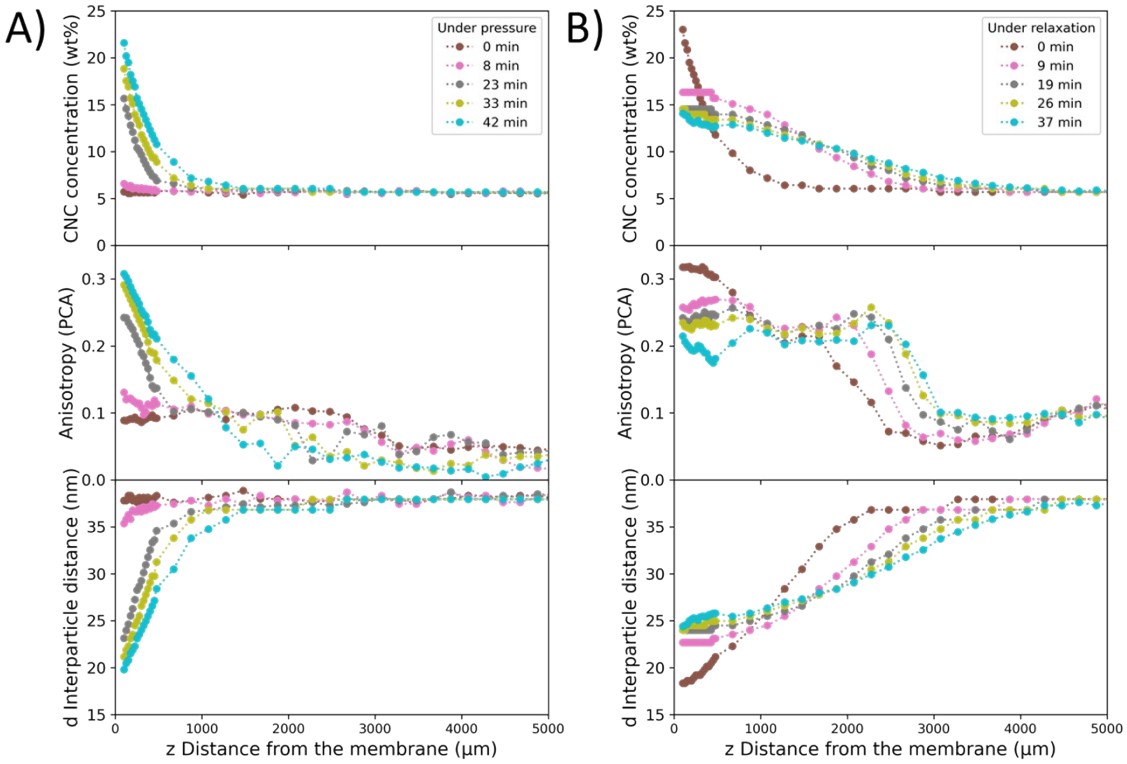

Figure S9: Evolution of CNC concentration, PCA anisotropy and interparticle distance during the filtration monitored by SAXS under pressure (A) and under relaxation (B).

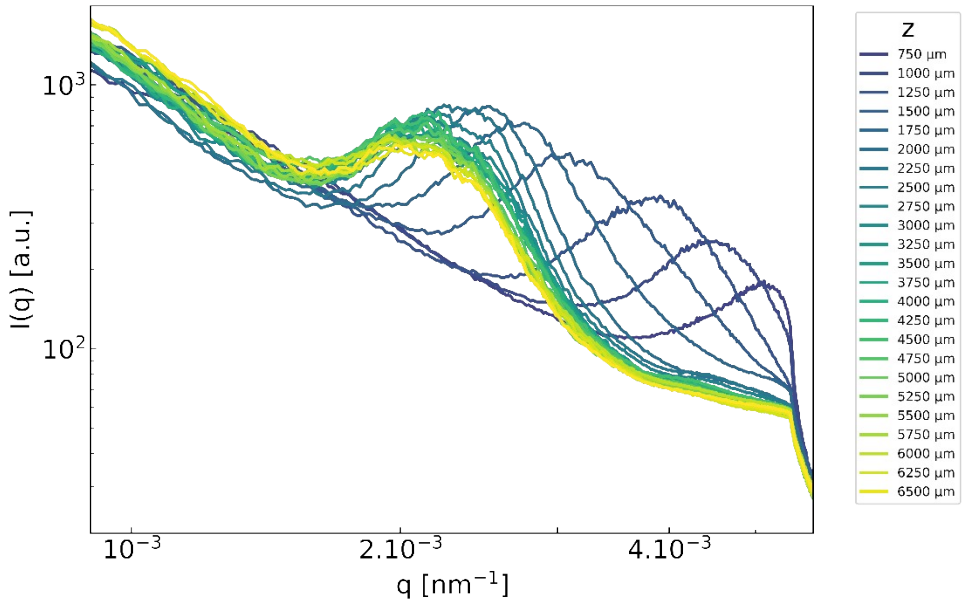

Figure S10: I(q) SALS curve: concentration profile at 222 min under pressure, 6 wt% CNCs.

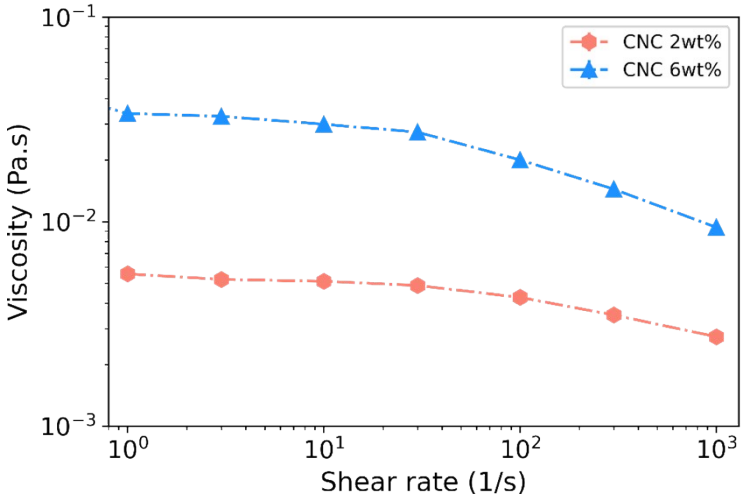

Figure S11: Flow curve of CNCs at 2 and 6 wt%.

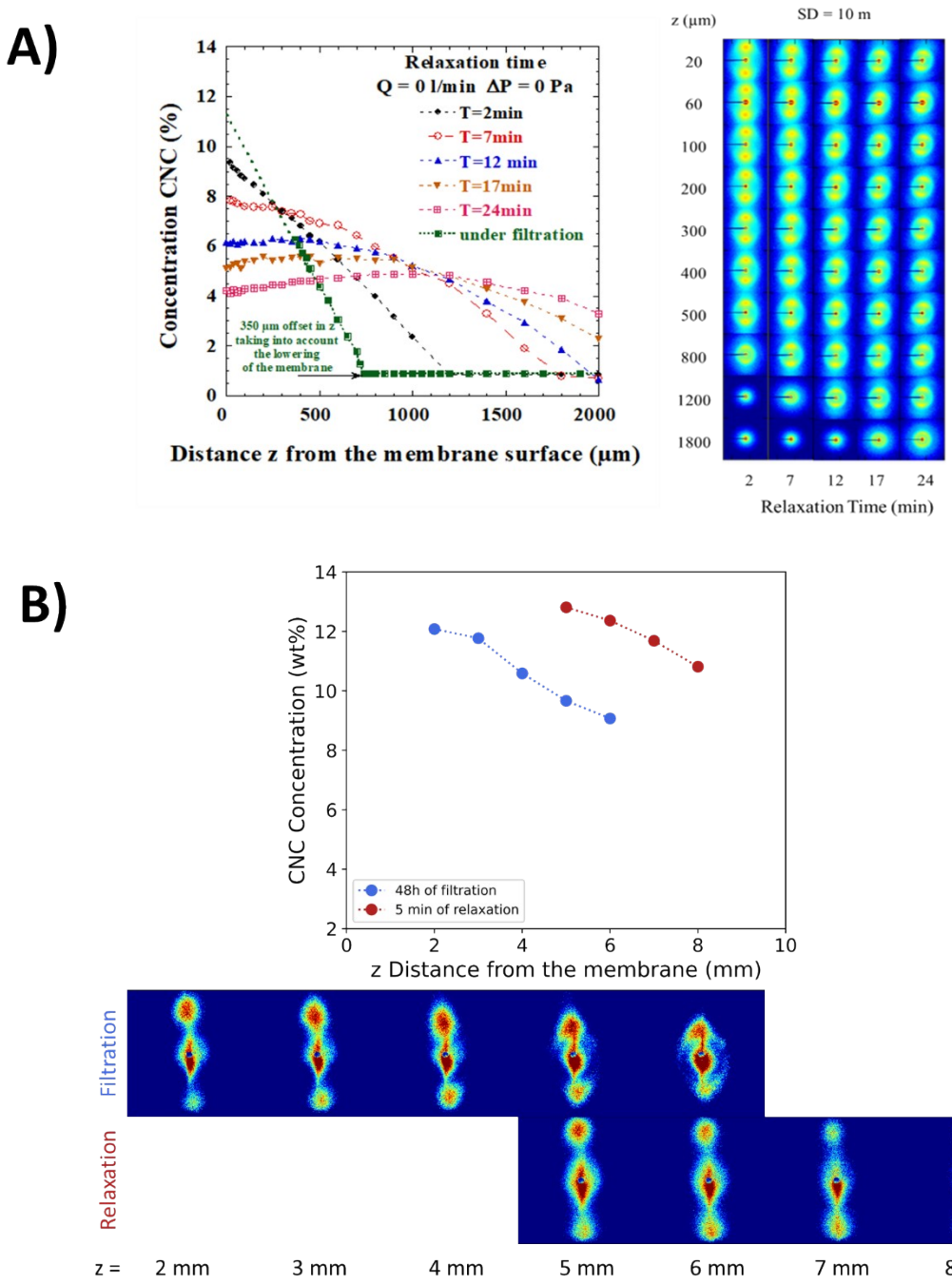

Figure S12: A) Concentration profile and associated scattering spectra measured during the 116 min filtration at ΔP = 1.2 × 10^5 Pa and a crossflow rate of 0.06 L.min^{-1} of a 0.7 wt% CNC suspension following with relaxation phase (at ΔP = 0 Pa and a crossflow rate of 0 L.min^{-1}) (ESRF report SC4177 and [66]). B) Concentration profile and SALS pattern after 48 h of filtration (at ΔP = 1.2 × 10^5 Pa) and after 5 min of the relaxation phase (at ΔP = 0 Pa) for a 2 wt% CNC suspension.

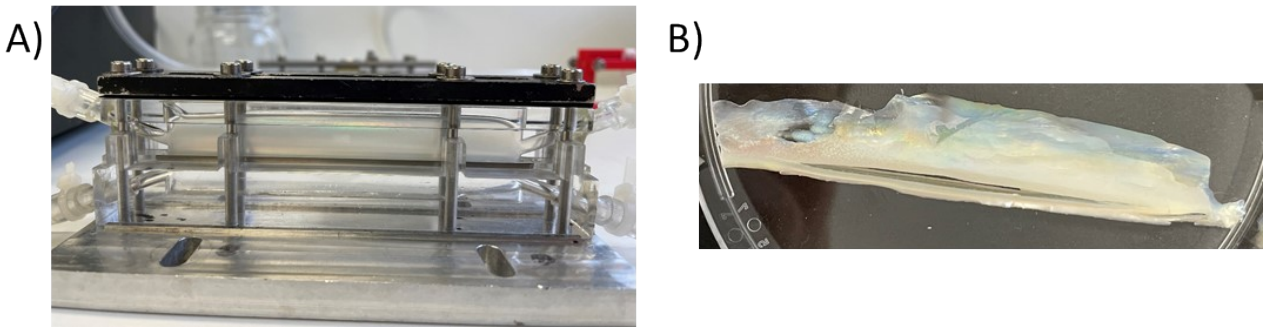

Figure S13: Photographs of the deposit in the filtration cell (A) and after drying (B).

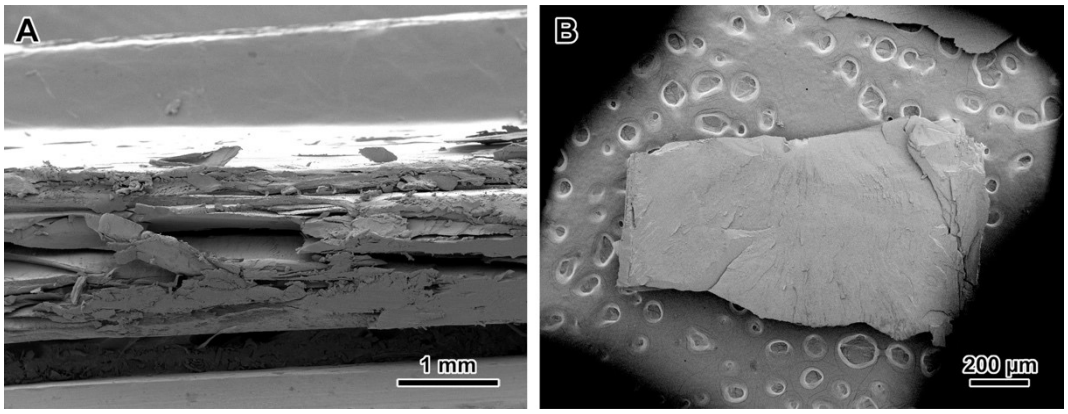

Figure S14: Low-magnification SEM images of two fragments prepared by fracturing the dry CNC deposit perpendicular (A) and parallel (B) to the surface.

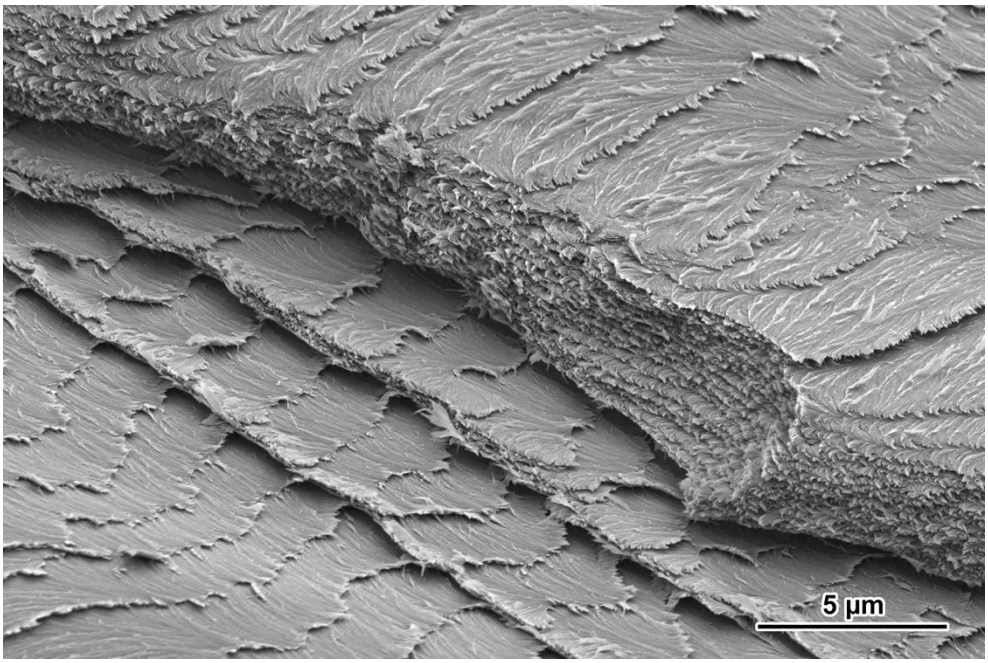

Figure S15: SEM images of the surface fracture of a fragment of dry CNC deposit exposing two types of fracture plane, one being mostly perpendicular and the other mostly parallel to the deposit surface.